A combined optimization of the sizing and the energy management of an industrial multi-energy microgrid: Application to a harbour area

Anthony Roy, Jean-Christophe Olivier, François Auger, Salvy Bourguet, Bruno Auvity, Emmanuel Schaeffer, Jacques Perret, Jonathan Schiebel

Energy Conversion and Management: X 12 (2021) 100107

Contents lists available at ScienceDirect

Energy Conversion and Management: X

journal homepage: www.sciencedirect.com/journal/energy-conversion-and-management-x

A combined optimization of the sizing and the energy management of an industrial multi-energy microgrid: Application to a harbour area

Anthony Roy [a,*], Jean-Christophe Olivier [a], François Auger [a], Bruno Auvity [b], Emmanuel Schaeffer [a], Salvy Bourguet [a], Jonathan Schiebel [c], Jacques Perret [d]

[a] Laboratoire IREENA, Université de Nantes, 37 Boulevard de l'Université, BP420, 44606 Saint-Nazaire cedex, France
[b] Laboratoire LTEN, Université de Nantes, La Chantrerie, rue Christian Pauc - CS 50609, 44306 Nantes cedex 3, France
[c] Akajoule, 18 bd Paul Perrin, 44600 Saint Nazaire cedex, France
[d] MAN Energy Solutions France, Avenue de Chatonay – Porte 7, BP427, 44615 Saint Nazaire cedex, France

ARTICLE INFO

Keywords:
Sizing optimization
Energy management optimization
Microgrid
Storage
Hydrogen

ABSTRACT

The current evolution of technical and environmental regulations and the recent development of hydrogen mobility require technological breakthroughs in the industrial areas, such as in harbours. Thus, multi-energy microgrids integrating low-carbon energy sources, electrical and hydrogen loads and storage solutions have to be designed. To improve their economic viability, the microgrid components must be carefully sized and the energy must be distributed in the most cost-effective way at any time. So as to foster the expansion of multi-energy microgrids in industrial areas, we propose in this paper a two-level optimization for the energy management and the sizing, applied to an original multi-energy scenario considering electricity and hydrogen as energy vectors. The designed energy management optimization takes into account an objective of economic profitability and constraints related to the availability of the sources and storage solutions, their reliability and the costs. The sizing optimization aims to propose different solutions allowing the benefits to be maximized and the expenses to be minimized. One of the main contributions of the paper is to compare the possible ways of valorisation of the energy available in an industrial microgrid. The results show that the sale of hydrogen allows income to be increased, in addition to self-consumption and sale to the electrical grid, but the electrolyzer involves high investments costs. Finally, a sensitivity analysis is presented and shows that the investment costs of electrolyzer and battery and the hydrogen selling price are key points in the optimal design.

1. Introduction

The recent environmental and technical regulations involve some changes in the design and management of electrical power grids in the harbour areas [1]. For example, the electrical power supply of berthed vessels by the onshore grid is more and more considered to limit the pollutants emitted by the vessel's engines [2]. Moreover, the seaports must adapt their electrical power system to the technological changes in the boats, as hybrid or fully-electric boats have been developed over the last years [3], mainly using energy storage solutions [4]. Furthermore, so as to limit the pollutants emission and the use of fossil fuels, the electrical power supply of the harbour's loads can be ensured by low-carbon energy sources, such as solar energy or wind energy [1]. Some energy can also be harnessed from different industrial processes [5], such as the seaport cranes [6] or the machine testing. On the other hand, the hydrogen is more and more considered in industrial and harbour areas, as the industrial processes requiring hydrogen are numerous and the integration of hydrogen in transport systems is under development, as for example in boats [7], hybrid vehicles and fuel cell electric vehicles [8]. In more and more cases, the hydrogen is generated thanks to renewable energy sources so as to decarbonize the hydrogen production [9]. The development of hydrogen fueling stations is also more and more discussed in the literature, investigating both design and sizing issues [10] but also management aspects [11]. The design of energy hubs in industrial and harbour areas is now a field of interest studied for example in [12], where the management of electrical, gas, heating and

* Corresponding author.
E-mail addresses: anthony.roy1@univ-nantes.fr (A. Roy), jean-christophe.olivier@univ-nantes.fr (J.-C. Olivier), francois.auger@univ-nantes.fr (F. Auger), bruno.auvity@univ-nantes.fr (B. Auvity), emmanuel.schaeffer@univ-nantes.fr (E. Schaeffer), salvy.bourguet@univ-nantes.fr (S. Bourguet), jonathan.schiebel@akajoule.com (J. Schiebel), jacques.perret@man-es.com (J. Perret).

https://doi.org/10.1016/j.ecmx.2021.100107
Received 15 July 2021; Received in revised form 27 August 2021; Accepted 28 August 2021
Available online 2 September 2021

cooling networks is investigated.

Thus, different energy sources and energy uses can be considered in a seaport area, which fosters the achievement of microgrids in seaports [5]. However, the renewable energy sources are non-dispatchable and the flexibility of harbour load demand is low as most of the loads are non-shiftable. Thus, storage solutions associated to an adapted energy management system are required to ensure that the load demand can be fully met. In addition to the operating aspects, the storage solutions must be carefully sized to cover the energy needs. The sizing must take into account the high investment costs, which is often a barrier for the integration of storage solutions in microgrids. Moreover, the sizing of a microgrid must consider the energy management strategy, which has a strong impact on the economical, the environmental and the reliability performances. This energy management can be designed thanks to different approaches as reviewed in [13]: rule-based algorithms, linear and non-linear programming, metaheuristics algorithms, etc. However, when a sizing optimization is computed, most of the papers consider a rule-based energy management algorithm due to computational time issues. The articles dealing with a combined optimization of sizing and energy management are less numerous. The relation between the sizing and operation optimizations for microgrids, and the possible optimization frameworks have been investigated in [14]. The energy management optimization is generally solved in an inner loop, considering operation costs and reliability aspects. The sizing optimization is solved in an upper level, taking into account the life cycle cost. Thus, the operation optimization is computed for each microgrid sizing proposed by the upper optimization level, which lengthens the computation time. A two-level optimization framework is proposed in [15,16] for a solar-hydrogen-battery stand-alone microgrid, considering a building load profile. The energy management problem is formulated as a linear problem, with a minimization of the operational costs, while the sizing optimization problem is solved thanks to a metaheuristic approach (genetic algorithm) to minimize life cycle cost. It can be noted that in these works, the load shedding is allowed but a penalty factor is considered. A similar combined optimization is proposed in [17], with a rolling horizon simulation and model predictive control approach for the energy management optimization. A two-level optimization is also proposed in [18], with a minimization of the annual cost in the outer loop (including investments) while the lower-level aims to minimize the levelized cost of hydrogen so as to promote hydrogen production. A two-stage optimization for a harbour microgrid has been proposed in [19], considering investments and planning optimization problems. The sizing optimization of all of these articles involves only one objective function. Nevertheless, the sizing optimization can also be formulated as a multi-objective optimization problem. In [20], a multi-objective sizing optimization is investigated, considering investments costs, levelized cost of energy and Diesel generator pollutant emission, while the operation optimization aims to determine the power dispatching allowing the operational cost to be minimized. The sizing optimization can be also formulated as a bi-objective problem, as for example in [21] where the net present cost and the carbon dioxide emission are minimized. However, such combined optimization problems lead to long computation time due to the simulation over a large data period and the complexity of solving linear programming problems. So as to reduce the computation time of the energy management optimization, a separation of the yearly profile into daily profiles has been proposed in [22]. It can be highlighted that both sizing and energy management optimization problems can also be integrated in a single optimization problem, as investigated in [23] for the design and the control of a hybrid vehicle. The control can involve a model predictive approach [24] and fuzzy logic rules [25].

From this review, it appears that the combined optimization of the sizing and the operation for industrial multi-energy microgrids is scarce in the literature. The existing papers have considered electrical power generation from renewable energy sources, but the existing industrial processes in industrial areas was not investigated. Moreover, the uncertainty about the hydrogen selling price appears to be a barrier and the design of economic regulation is still under study [26]. So as to foster the development of microgrids in industrial areas, it is necessary to compare the possible means of valorisation and quantify their costs and their benefits, which has not yet been deeply investigated in the literature. Thus, this paper proposes a combined optimization of the sizing and of the energy management applied to an industrial multi-energy microgrid. The proposed study deals with the case study of a harbour area as the possibilities of energy recovery are numerous, such as renewable energy sources and industrial processes, with a high amount of energy and high power level. Moreover, the hydrogen needs are growing as the maritime and terrestrial mobility considers more and more the hydrogen energy vector, so a low-cost hydrogen production from low-carbon energy is often expected by the seaports. In this article, several ways of energy valorisation are considered and compared, in order to optimize the use of the energy available in the seaport. The generated electrical energy can be valued either by self-consumption or by feeding into the main electrical network. It can also be converted into hydrogen, used for harbour loads (mobility and industrial processes) or fed into an external gas network. To allow the generated energy to be used later, batteries and hydrogen tank storage solutions are considered. The investigated case study is based on an actual scenario, developed in the context of a national French project, ESTUAIRE [27], which deals with the economic potential of a Smart Grid approach in industrial and seaport areas. This project mainly involves harbour industrials, such as ship and high power engine builders. Thus, the modeling and optimization methodology proposed in this paper is applied to a harbour application case, but it could be also applied to any industrial area where a multi-energy microgrid is considered. It can be highlighted that the approaches and solving tools we have used for the optimization of both energy management and sizing have already been used in the literature for other kinds of problems, showing then their effectiveness. The novelty of the study presented in this article concerns the industrial application framework and the related optimization problem formalization. In summary, the main contributions of this paper are:

- A two-level sizing and energy management optimization of a multi-energy industrial microgrid, including the comparison of different ways of valorisation (self-consumption, electricity and hydrogen sales), in order to determine how the available energy has to be shared;
- A multi-use of hydrogen, namely gas network injection and local use for mobility and industrial processes, according to different selling prices assumptions;
- The self-discharge of the storage devices and the operational costs are taken into account in the energy management problem;
- A study of the consequences of the uncertainties of the hydrogen selling price and investment costs on the results.

The paper is organized as follows. Section 2 presents the system modeling. The two-level optimization is described in the Section 3. In the Section 4, energy management and sizing results are presented, in addition to a sensitivity analysis about the economic parameters. Section 5 concludes the paper.

2. Harbour microgrid modeling

The harbour microgrid studied in this paper is made of different elements related to power generation, energy storage, loads and connections to the electrical grid and to a gas network. An overview of this microgrid is shown in Fig. 1, considering a power flow modeling.

The electrical energy can be generated in the harbour area thanks to solar photovoltaic panels. Moreover, the testing of generators manufactured in the harbour is also considered as a power source. An electrical power is generated by the engine during the validation tests and fed into the grid. The total power generated from these two kinds of non-dispatchable energy sources is denoted as P_{gen} [W]. Several uses are

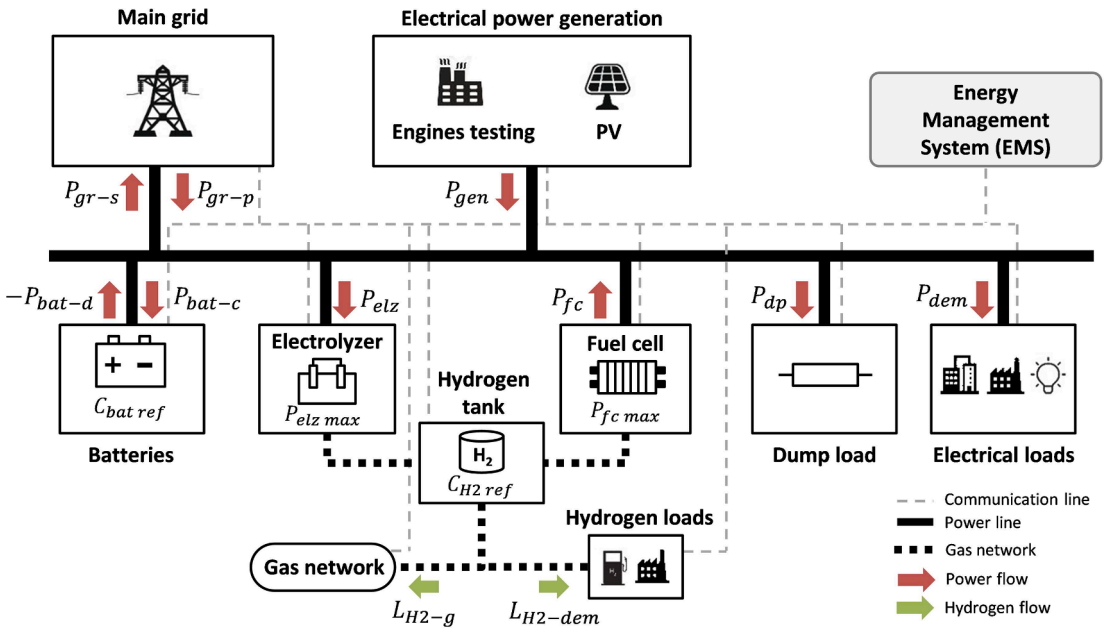

Fig. 1. Overview of the considered industrial multi-energy microgrid.

considered: the generated power P_{gen} can be fed into the electrical main grid (P_{gr-s}), or converted into hydrogen thanks to an electrolyzer (P_{elz}), or used for the supply of the electrical loads (P_{dem}). The harnessed energy from these sources can also be stored into batteries or a hydrogen tank so as to be used later. The produced hydrogen can be either fed into gas network (L_{H2-g}) or used for the supply of the hydrogen load demand of the harbour area (L_{H2-dem}). The considered hydrogen loads are related to the industrial needs (engines testing) and the mobility needs (fleet of vehicles including cars, buses and boats). This hydrogen can also be used to generate electrical power thanks to a fuel cell (P_{fc}). Finally, the hydrogen can be produced thanks to power drawn from the main grid, to allow hydrogen demand to be met if the power generation from local energy sources is low, or if hydrogen production is profitable according to electricity purchase price. The total demanded electrical power of the considered harbour microgrid is denoted as P_{dem} [W]. This power includes the power consumption of industrial buildings in the harbour area and also seaport basins pumps. It can be noted that no load shedding is considered, thus the power P_{dem} and the hydrogen load demand L_{H2-dem} have to be met all the time, supplied by microgrid components or by purchasing electricity from main grid (P_{gr-p}). In case of power congestion, i.e. when the generated power is larger than the demanded power and the valorisation solutions are used at the maximum allowed power, the surplus of generated power is dissipated into a dump load (P_{dp}). The models and the details related to the storage solutions are given in the following sections.

2.1. Battery model

The use of batteries is considered so as to supply the loads in case of low generated power or to later feed energy into external networks, at a time where the selling price is higher. The batteries model is based on the calculation of the state of charge *SoC* at each time sample t_k, by taking the efficiency in charge and discharge and the self-discharge of the batteries into account [28–30]:

$$SoC(t_k) = \alpha_{bat} SoC(t_{k-1}) + \frac{\Delta t}{C_{batref}} \left(\eta_{bat-c} P_{bat-c}(t_{k-1}) + \frac{P_{bat-d}(t_{k-1})}{\eta_{bat-d}} \right) \quad (1)$$

where C_{batref} is the nominal capacity of the batteries [Wh], P_{bat-c} the operating power of the batteries in charge [W] considered as positive, P_{bat-d} the operating power of the batteries in discharge [W] considered as negative, Δt the time step [h], α_{bat} the self-discharge coefficient, η_{bat-c} the batteries efficiency in charge and η_{bat-d} the batteries efficiency in discharge. The self-discharge coefficient α_{bat} is calculated from the daily self-discharge rate σ_{bat} [%/day] by:

$$\alpha_{bat} = (1 - \sigma_{bat})^{\frac{\Delta t}{24}} \quad (2)$$

2.2. Hydrogen storage model

The energy generated by the sources in the harbour area can be valued by producing hydrogen thanks to an electrolyzer. The hydrogen can be fed into the gas network (Power-to-Gas valorisation), or used to supply the hydrogen demand or used later to produce electrical energy through a fuel cell (Gas-to-Power valorisation). Thus, a hydrogen tank is considered in this study to meet the hydrogen storage needs. The hydrogen storage model is based on the calculation of the level of hydrogen *LoH* at each time sample t_k [30]:

$$LoH(t_k) = \alpha_{H2} LoH(t_{k-1}) + \frac{\Delta t}{C_{H2ref}} \left(\eta_{elz} P_{elz}(t_{k-1}) - \frac{P_{fc}(t_{k-1})}{\eta_{fc}} - \left(L_{H2-g}(t_{k-1}) + L_{H2-dem}(t_{k-1}) \right) \gamma_{H2} \right) \quad (3)$$

where C_{H2ref} is the capacity of the hydrogen tank [Wh], L_{H2-dem} the hydrogen volume flow rate fed into the harbour hydrogen distribution network [Nm^3/h, normal cubic meter per hour] which corresponds to the hydrogen mobility and industrial demand, L_{H2-g} the hydrogen volume flow rate fed into the external gas network [Nm^3/h], P_{elz} the operating power of the electrolyzer [W], P_{fc} the operating power of the

fuel cell [W], α_{H2} the self-discharge coefficient, γ_{H2} the conversion factor between hydrogen volume and hydrogen energy ($\gamma_{H2} = 3000$ Wh/Nm^3), η_{elz} the electrolyzer efficiency and η_{fc} the fuel cell efficiency. As for the battery, the self-discharge coefficient α_{H2} (which corresponds to the leakages in the hydrogen tank) is calculated from the daily self-discharge rate σ_{H2} [%/day] by:

$$\alpha_{H2} = (1 - \sigma_{H2})^{\frac{\Delta t}{24}} \quad (4)$$

3. Two-level optimization problem

First, a sizing optimization is necessary to determine the capacity of both storage solutions and the nominal powers of the electrolyzer and of the fuel cell, allowing the load demand to be met while minimizing their costs. Moreover, an optimization of the energy management is required as the considered microgrid studied in this paper is composed of two storage solutions and of different ways of valorisation governed by constant or variable prices. Thus, a combined optimization of the energy management and the sizing for the considered application framework is proposed, by using methods and tools which have been investigated in several papers as discussed in the literature survey in Section I. An overview of the considered two-level optimization is given in Fig. 2. The outer loop of the optimization scheme is related to the sizing. It aims to determine a panel of optimal solutions (located on a Pareto front) allowing to get the maximum annual net income $c_{netinc/y}$ for a minimum life cycle cost c_{LCC}. For each configuration generated in the sizing optimization algorithm, a simulation of the operation profile is done, considering an optimization of the energy management (inner loop). The aim of this inner loop is to determine the operation profile of each component allowing a sum of operating costs to be minimized, considering expenses and incomes. The input data of this combined optimization are related to economic and technical parameters, in addition to the load demand and the generated power profiles. Both optimization problems are described in the following sections, according to the objective function, the decision variables and the constraints.

3.1. Energy management optimization problem

The energy management problem is formulated as an optimization problem so as to obtain the best power profile for each component over a given period, according to a desired objective. The operation strategy for each component over a given period can be determined from the current state of the system and the power generation, load demand and selling prices for the coming period. The optimization problem is written as a Mixed Integer Linear Programming (MILP) problem. This method is widely used in the literature for the optimization of energy management [12,15,21]. In this paper, we show how to apply this approach to the original framework of an industrial microgrid, considering multiple energy vectors. The decision variables, the objective function and the constraints of this unit commitment problem are described in the following subsections.

3.1.1. Decision variables

For the inner loop, related to the energy management, the decision variables considered for the optimization problem are related to the operation of each microgrid element. Thus, a total of ten decision variables are considered at each time sample t_k, with X_k and X the set of decision variables for the time t_k and for the whole period of K time samples:

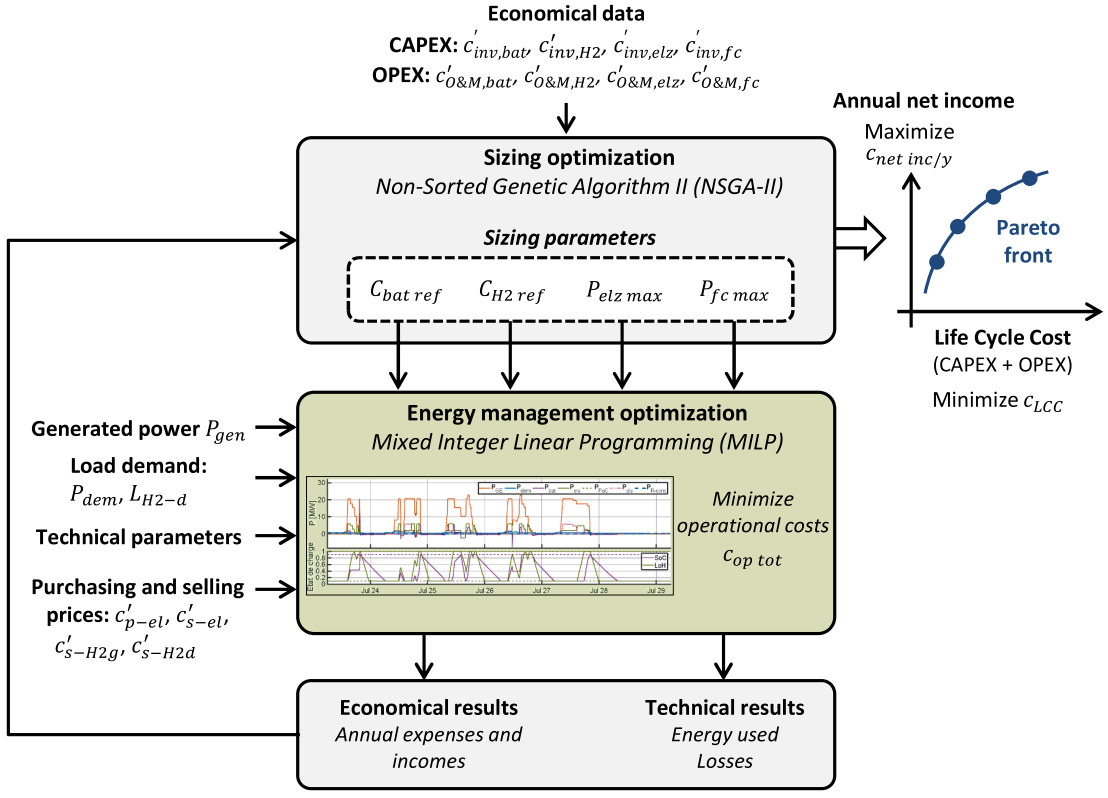

Fig. 2. Framework of the two-level optimization, with energy management optimization and sizing optimization.

$$X_k = \left\{P_{gr-s}(t_k), L_{H2-g}(t_k), P_{bat-c}(t_k), P_{bat-d}(t_k), b_{bat-c}(t_k), P_{elz}(t_k), P_{fc}(t_k), P_{dp}(t_k), P_{gr-p/el}(t_k), P_{gr-p/H2}(t_k)\right\} \quad (5)$$

$$X = \{X_1, \cdots, X_k, \cdots, X_K\}, 1 \leq k \leq K, k, K \in \mathbb{N} \quad (6)$$

$$P_{gr-s}(t_k), L_{H2-g}(t_k), P_{bat-c}(t_k), P_{bat-d}(t_k), P_{elz}(t_k), P_{fc}(t_k), P_{dp}(t_k), P_{gr-p/el}(t_k), P_{gr-p/H2}(t_k) \in \mathbb{R} \quad (7)$$

$$b_{bat-c}(t_k) \in \{0; 1\} \quad (8)$$

where P_{gr-s} is the power fed into the electrical grid corresponding to the electricity selling [W], L_{H2-g} the hydrogen volume flow rate fed into the gas network [Nm^3/h], P_{bat-c} the operating power of the batteries in charge [W],P_{bat-d} the operating power of the batteries in discharge [W], b_{bat-c} a binary variable allowing the batteries to be used either in charge ($b_{bat-c} = 1$) or in discharge ($b_{bat-c} = 0$), P_{elz} the operating power of the electrolyzer [W], P_{fc} the operating power of the fuel cell [W], P_{dp} the power dissipated into the dump load [W], $P_{gr-p/el}$ the power drawn from main grid so as to ensure all the electrical load demand is met [W] and $P_{gr-p/H2}$ the power drawn from main grid for hydrogen production [W]. It can be noted that the sum of these last two powers ($P_{gr-p/el} + P_{gr-p/H2}$) corresponds to the total power P_{gr-p} drawn from the main grid (Fig. 1).

3.1.2. Objective function

The goal of the optimization problem is to minimize the sum of operating costs over a given period, considering the expenses and the incomes. The total operation cost c_{optot} over a period of K time samples is defined by:

$$c_{optot} = \Delta t \sum_{k=1}^{K} c'_{s-el}(t_k) P_{gr-s}(t_k) + c'_{s-H2g}(t_k) L_{H2-g}(t_k) + c'_{op-bat}(t_k) P_{bat-c}(t_k) - c'_{op-bat}(t_k) P_{bat-d}(t_k) + c'_{op-elz}(t_k) P_{elz}(t_k) + c'_{op-fc}(t_k) P_{fc}(t_k) + c'_{p-el}(t_k) P_{gr-p/el}(t_k) + c'_{p-el}(t_k) P_{gr-p/H2}(t_k) \quad (9)$$

where c_{optot} is the total operating cost over the period [€], c'_{s-el} the electricity selling price [€/Wh], c'_{s-H2g} the selling price of hydrogen fed into gas network [€/Nm^3], c'_{op-bat} the operating cost of the batteries [€/Wh], c'_{op-elz} the operating cost of the electrolyzer [€/Wh], c'_{op-fc} the operating cost of the fuel cell [€/Wh] and c'_{p-el} the electricity purchase price [€/Wh].

So as to minimize this objective function, the incomes obtained from the sale of electricity and hydrogen are considered to be negative (c'_{s-el} and c'_{s-H2g}), whereas the expenses related to the operation of devices (c'_{op-bat}, c'_{op-elz} and c'_{op-fc}) and the purchase of electricity (c'_{p-el}) are considered to be positive.

3.1.3. Constraints

A set of constraints is considered in the optimization problem so as to obtain a feasible solution. The first constraint is related to the power balance which must be met at each time sample t_k, so as to ensure all the demand is supplied:

$$P_{gen}(t_k) + P_{gr-p/el}(t_k) + P_{gr-p/H2}(t_k) + P_{fc}(t_k) - P_{bat-d}(t_k) = P_{gr-s}(t_k) + P_{bat-c}(t_k) + P_{elz}(t_k) + P_{dp}(t_k) + P_{dem}(t_k) \quad (10)$$

The operating limits of each component must be taken into account, such as the power limits but also the minimum and maximum values of state of charge. Thus, the following decision variables are constrained by:

$$0 \leq P_{gr-s}(t_k) \leq P_{gr-smax} \quad (11)$$

$$0 \leq L_{H2-g}(t_k) \leq L_{H2-gmax} \quad (12)$$

$$0 \leq P_{elz}(t_k) \leq P_{elzmax} \quad (13)$$

$$0 \leq P_{fc}(t_k) \leq P_{fcmax} \quad (14)$$

$$0 \leq P_{dp}(t_k) \leq P_{dpmax} \quad (15)$$

The power drawn from the electrical main grid $P_{gr-p/el}$ cannot overpass the sum of electrical load demand and the batteries charging power (eq. (16)), so as to ensure that batteries self-discharge can be compensated whatever the generated power. The power drawn from the electrical main grid $P_{gr-p/H2}$ cannot overpass the electrolyzer power (eq. (17)).

$$0 \leq P_{gr-p/el}(t_k) \leq P_{dem}(t_k) + P_{bat-c}(t_k) \quad (16)$$

$$0 \leq P_{gr-p/H2}(t_k) \leq P_{elz}(t_k) \quad (17)$$

The decision variables related to the batteries operation must also meet some constraints. Indeed, the batteries cannot operate simultaneously in charge and discharge, thus the equation $P_{bat-c}(t_k) \times P_{bat-d}(t_k) = 0$ must be verified at each time sample. So as to transform this constraint into a linear constraint, the binary variable b_{bat-c} is integrated in the optimization problem thanks to the following equations [31]:

$$0 \leq P_{bat-c}(t_k) \leq b_{bat-c}(t_k) P_{bat-cmax} \quad (18)$$

$$(1 - b_{bat-c}(t_k)) P_{bat-dmin} \leq P_{bat-d}(t_k) \leq 0 \quad (19)$$

$$0 \leq b_{bat-c}(t_k) \leq 1, b_{bat-c}(t_k) \in \mathbb{N} \quad (20)$$

Moreover, the state of charge of the batteries and the level of hydrogen in the hydrogen tank are constrained by lower and upper limits:

$$SoC_{min} \leq SoC(t_k) \leq SoC_{max} \quad (21)$$

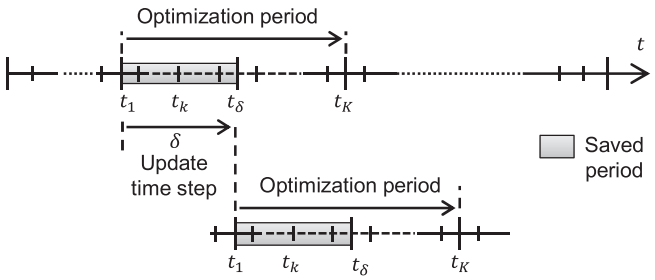

Fig. 3. Timeline of the simulation scheduling with rolling horizon.

$$LoH_{min} \leq LoH(t_k) \leq LoH_{max} \tag{22}$$

At each time sample t_k, the state of charge of the batteries SoC can be formulated as a linear combination of the charge power and the discharge power since the beginning of the considered period (time sample t_1):

$$SoC(t_k) = SoC(t_1)\alpha_{bat}{}^{k-1} + \frac{\Delta t}{C_{batref}} \sum_{i=1}^{k-1} \alpha_{bat}{}^{k-1-i} \left(P_{bat-c}(t_i)\eta_{bat-c} + \frac{P_{bat-d}(t_i)}{\eta_{bat-d}} \right) \tag{23}$$

The same principle can be applied for the level of hydrogen of the hydrogen tank:

$$LoH(t_k) = LoH(t_1)\alpha_{H2}{}^{k-1} + \frac{\Delta t}{C_{H2ref}} \sum_{i=1}^{k-1} \alpha_{H2}{}^{k-1-i} \left(P_{elz}(t_i)\eta_{elz} - \frac{P_{fc}(t_i)}{\eta_{fc}} - \left(L_{H2-g}(t_i) + L_{H2-dem}(t_i) \right)\gamma_{H2} \right) \tag{24}$$

So as to start each day with an optimal level of hydrogen stored into the tank, allowing the hydrogen load demand to be supplied, an additional constraint has been added to the energy management problem. This constraint consists in imposing that the level of hydrogen LoH must be at its maximum level at 6 a.m.:

$$LoH(t = 6a.m.) = LoH_{max} \tag{25}$$

3.1.4. Optimization problem solving

The optimization problem related to the energy management can be formulated as a MILP optimization problem, considering equality and inequality constraints, such as:

$$\min_X \left(c_{optot} \right) \text{s.t.} (10) - (25) \tag{26}$$

This MILP optimization problem is solved with the *intlinprog* function available in MATLAB software (Optimization Toolbox) [32], as the optimization problem to be solved is linear (objective function and constraints) and some of the decision variables are integer variables. This solving tool considers a branch-and-bound algorithm to solve the optimization problem. The implemented objective function corresponds to the equation (9), related to the minimization of the total operational cost. The equality and inequality constraints described in the equations (10)-(25) are implemented in matrix form.

So as to limit the computation time due to a high number of time samples, increasing the size of the MILP optimization problem, the energy management optimization problem is solved using a rolling horizon simulation, considering consecutive periods of several hours and an update time step δ as shown in Fig. 3. This concept of rolling horizon simulation with an update time step is explained in [33,34]. Only the first δ time samples are kept at each optimization and the rest of the period is re-evaluated in the next optimization, according to the power generation and demand of the K new incoming hours. The choice of the values of δ and K must allow that the operating decisions taken during the first δ time samples of the optimization period have no influence on what can happen after the end of the optimization period.

3.2. Sizing optimization problem

The outer loop of the two-level optimization process is related to the sizing optimization. This optimization problem aims to define the size of the devices allowing the operation costs to be minimized as much as possible through the energy management optimization problem presented previously (inner loop), while minimizing the life cycle cost of the configuration through the sizing optimization (outer loop) [15,17,18].

3.2.1. Decision variables

The devices parameters to be sized are the batteries capacity C_{batref}, the hydrogen tank capacity C_{H2ref}, the electrolyzer maximum power P_{elzmax} and the fuel cell maximum power P_{fcmax}. The vector S represents the set of decision variables related to the sizing optimization problem:

$$S = \left\{ C_{batref}, C_{H2ref}, P_{elzmax}, P_{fcmax} \right\} \tag{27}$$

It can be noted that the size of the other components of the microgrid is imposed: the dump load maximum power P_{dpmax}, the main grid maximum power $P_{gr-smax}$ and the maximum hydrogen flow rate fed into the gas network $L_{H2-gmax}$. The installed power of solar photovoltaic panels is also imposed and defined according to the available area on the roofs of the seaport buildings. Indeed, in this case study, the PV array does not need to be sized by an optimization since the minimum possible amount of demanded energy per day is larger than the maximum possible amount of energy generated by this PV array per day. It is also more profitable to use the energy generated by a PV array than to purchase electricity to the grid.

3.2.2. Objective functions

So as to propose a set of the best solutions and offer a tradeoff between expenses and incomes, a bi-objective optimization problem is considered for the sizing optimization. Thus, the aim of the optimization tool is to find the Pareto-front allowing the expenses to be minimized and the incomes to be maximized.

The first objective is related to the minimization of the total expenses over the life cycle of the system c_{LCC} [€], including investment and maintenance costs for each component over the system lifetime [35] and defined as:

$$c_{LCC} = c_{invtot} + \sum_{i=1}^{N_{life}} \frac{c_{O\&Mtot/y}}{(1+d)^i} \tag{28}$$

$$c_{invtot} = c'_{inv,bat} C_{batref} + c'_{inv,H2} C_{H2ref} + c'_{inv,elz} P_{elzmax} + c'_{inv,fc} P_{fcmax} + c_{inv,PV} + c_{inv,gr} + c_{inv,dp} \tag{29}$$

$$c_{O\&Mtot/y} = c'_{O\&M,bat} C_{batref} + c'_{O\&M,H2} C_{H2ref} + c'_{O\&M,elz} P_{elzmax} + c'_{O\&M,fc} P_{fcmax} + c_{O\&MPV} \tag{30}$$

where c_{invtot} is the total investment costs [€], $c'_{inv,bat}$ the batteries investment costs [€/Wh], $c'_{inv,H2}$ the hydrogen tank investment cost [€/Wh], $c'_{inv,elz}$ the electrolyzer investment cost [€/W], $c'_{inv,fc}$ the fuel cell investment cost [€/W], $c_{inv,PV}$ the solar photovoltaic panels investment cost [€], $c_{inv,gr}$ the grid connection investment cost [€], $c_{inv,dp}$ the dump load investment cost [€], $c_{O\&Mtot/y}$ the yearly total operational and maintenance (O&M) costs [€/y], $c'_{O\&M,bat}$ the O&M battery cost [€/Wh/y], $c'_{O\&M,H2}$ the O&M hydrogen tank cost [€/Wh/y], $c'_{O\&M,elz}$ the electrolyzer O&M cost [€/W/y], $c'_{O\&M,fc}$ the fuel cell O&M cost [€/W/y], $c_{O\&MPV}$ the solar photovoltaic panels O&M cost [€/y], d the real discount rate and N_{life} the lifetime of the system [years]. It can be noted that the replacement costs are included in the second objective function, as they are related to the operational strategies.

The second objective of the sizing optimization problem is related to the maximization of the annual net income $c_{netinc/y}$ [€], considered as positive, defined as the difference between the annualized incomes and variable expenses:

$$c_{netinc/y} = c_{s-el/y} + c_{s-H2g/y} + c_{s-H2dem/y} + c_{s-c/y} - c_{repbat/y} - c_{repelz/y} - c_{repfc/y} - c_{p-elH2/y} \tag{31}$$

where $c_{s-el/y}$ is the annual income brought by the sale of electricity [€/y], defined as follows for a simulation over a period of N_{ysim} years, composed of N time samples:

$$c_{s-el/y} = -\frac{\Delta t}{N_{ysim}} \sum_{k=1}^{N} c'_{s-el}(t_k) P_{gr-s}(t_k) \tag{32}$$

The cost $c_{s-H2g/y}$ is the annual income brought by the sale of hydrogen fed into gas network [€/y], defined as:

$$c_{s-H2g/y} = -\frac{\Delta t}{N_{ysim}} \sum_{k=1}^{N} c'_{s-H2g}(t_k) L_{H2-g}(t_k) \tag{33}$$

The cost $c_{s-H2dem/y}$ is the annual income brought by the sale of hydrogen for the supply of the harbour area demand [€/y], defined as:

$$c_{s-H2dem/y} = -\frac{\Delta t}{N_{ysim}} \sum_{k=1}^{N} c'_{s-H2dem}(t_k) L_{H2-dem}(t_k) \tag{34}$$

with $c'_{s-H2dem}$ the selling price of hydrogen for mobility and industrial processes [€/Nm^3], considered as negative.

The cost $c_{s-c/y}$ is the annual income brought by the electricity purchase savings [€/y], corresponding to the self-consumption, defined as:

$$c_{s-c/y} = \frac{\Delta t}{N_{ysim}} \sum_{k=1}^{N} c'_{p-el}(t_k) \left(P_{dem}(t_k) - P_{gr-p/el}(t_k) \right) \tag{35}$$

The cost $c_{repbat/y}$ corresponds to the batteries annualized replacement cost [€/y]. It is annualized according to estimated battery lifetime, which depends on the battery use over the simulated period:

$$c_{repbat/y} = \frac{c'_{inv,bat} C_{batref} \Delta t}{E_{batexc} N_{ysim}} \sum_{k=1}^{N} |P_{bat-c}(t_k) + P_{bat-d}(t_k)| \tag{36}$$

where E_{batexc} is the maximum exchangeable energy of the battery during its lifetime before replacement [Wh].

The cost $c_{repelz/y}$ represents the electrolyzer annualized replacement cost [€/y], evaluated from the simulation thanks to:

$$c_{repelz/y} = \frac{c'_{inv,elz} P_{elzmax} \Delta t}{N_{helzmax} N_{ysim}} \sum_{k=1}^{N} b_{elz}(t_k) \tag{37}$$

$$b_{elz}(t_k) = \begin{cases} 1, & \text{if } P_{elz}(t_k) > 0 \\ 0, & \text{otherwise} \end{cases} \tag{38}$$

where $N_{helzmax}$ is the maximum operating hours of the electrolyzer over its lifetime before considering replacement and $b_{elz}(t_k)$ a binary variable defining if the electrolyzer is operating or not.

As for the electrolyzer, the cost $c_{repfc/y}$ represents the fuel cell annualized replacement cost [€/y], evaluated from the simulation thanks to:

$$c_{repfc/y} = \frac{c'_{inv,fc} P_{fcmax} \Delta t}{N_{hfcmax} N_{ysim}} \sum_{k=1}^{N} b_{fc}(t_k) \tag{39}$$

$$b_{fc}(t_k) = \begin{cases} 1, & \text{if } P_{fc}(t_k) > 0 \\ 0, & \text{otherwise} \end{cases} \tag{40}$$

where N_{hfcmax} is the maximum operating hours of the fuel cell over its lifetime before considering replacement and $b_{fc}(t_k)$ a binary variable defining if the fuel cell is operating or not.

The cost $c_{p-elH2/y}$ represents the annual purchasing cost of electricity for H_2 production [€/y], defined as:

$$c_{p-elH2/y} = \frac{\Delta t}{N_{ysim}} \sum_{k=1}^{N} c'_{p-el}(t_k) P_{gr-p/H2}(t_k) \tag{41}$$

Thus, the first objective function (28) is only related to the sizing of the components, while the second objective function (31) depends on both the energy management optimization results and the sizing.

Table 1
Technical parameters.

Parameter	Value
E_{batexc}	13.734 GWh for C_{batref} = 1.09 MWh
$L_{H2-gmax}$	200 Nm^3/h
LoH_{max}	1
LoH_{min}	0.1
LoH_{init}	0.1
$N_{helzmax}$	60 000 h
N_{hfcmax}	30 000 h
$P_{bat-cmax}$	2.2 MW for a battery of C_{batref} = 1.09 MWh
$P_{bat-dmax}$	− 2.2 MW for a battery of C_{batref} = 1.09 MWh
P_{dpmax}	26 MW
$P_{gr-smax}$	12 MW
SoC_{max}	0.9
SoC_{min}	0.1
SoC_{init}	0.1
γ_{H2}	3000 Wh/Nm^3
η_{bat-c}	96 %
η_{bat-d}	96 %
η_{elz}	70 %
η_{fc}	50 %
σ_{bat}	0.17 %/d
σ_{H2}	0.01 %/d
K	192 (corresponding to 48 h for Δt = 15 min)
N	35,040 (simulation over one year with Δt = 15 min)
N_{life}	25
N_{ysim}	1
Δt	15 min
δ	96 (corresponding to 24 h for Δt = 15 min)

Table 2
Economic parameters.

Parameter	Value
$c'_{inv,bat}$	350 €/kWh
$c'_{inv,elz}$	1500 €/kW
$c'_{inv,fc}$	2500 €/kW
$c'_{inv,H2}$	20 €/kWh
$c'_{O\&M,bat}$	6 €/kWh/y
$c'_{O\&M,elz}$	67.5 €/kW/y
$c'_{O\&M,fc}$	75 €/kW/y
$c'_{O\&M,H2}$	0.2 €/kWh/y
c'_{op-bat}	0.02 €/kWh
c'_{op-elz}	0.005 €/kWh
c'_{op-fc}	0.01 €/kWh
$c_{inv,dp}$	1.5 M€
$c_{inv,gr}$	2 M€
$c_{inv,PV}$	4.32 M€
$c_{O\&M,PV}$	60.4 k€/y
d	5 %
PP_{max}	20 years

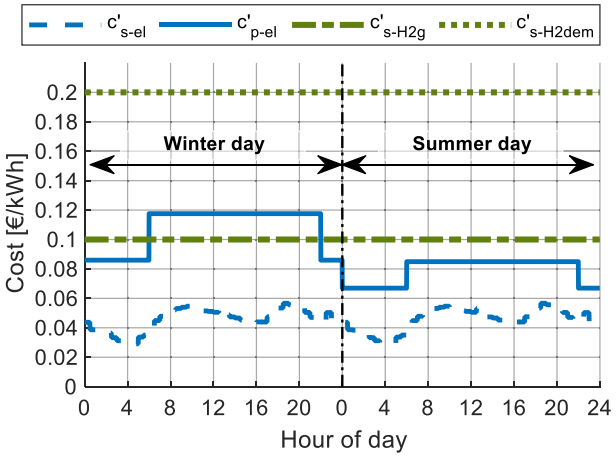

Fig. 4. Energy selling and purchasing prices over a "winter" day (31st March) and a "summer" (1st April) day.

3.2.3. Constraints

The optimal solutions must satisfy several constraints. The first kind of constraints is related to the lower and upper boundaries of each decision variable:

$$C_{batref,low} \leq C_{batref} \leq C_{batref,up} \quad (42)$$

$$C_{H2ref,low} \leq C_{H2ref} \leq C_{H2ref,up} \quad (43)$$

$$P_{elzmax,low} \leq P_{elzmax} \leq P_{elzmax,up} \quad (44)$$

$$P_{fcmax,low} \leq P_{fcmax} \leq P_{fcmax,up} \quad (45)$$

It can be noted that these upper limits are related to the available area in the harbour which could be used to set up the microgrid devices.

Moreover, the payback period PP of the sizing cannot overpass an upper limit PP_{max} so as to be realistic [36]:

$$PP = \frac{c_{invtot}}{c_{netinc/y} - c_{O\&Mtot/y}}, 0 \leq PP \leq PP_{max} \quad (46)$$

3.2.4. Optimization problem solving

The optimization problem related to the sizing can be formulated as a bi-objective problem for which two conflicting objectives have to be minimized, summarized as:

$$\min_{S}\left(c_{LCC}, -c_{netinc/y}\right) \text{s.t.} (42) - (46) \quad (47)$$

The sizing optimization problem is solved thanks to a metaheuristic approach, using a genetic algorithm called Nondominated Sorting Genetic Algorithm (NSGA-II) and developed by K. Deb et al. [37]. This tool has been widely used for solving complex bi-objective sizing optimization problems [21,38], so as to determine the best configurations according to two conflictive objectives. It is suitable for the solving of optimization problems with large search space and non-linear characteristics, which is the case of the presented optimization problem. Other optimization algorithms could be used to solve the considered optimization problem, but the comparison of optimization tools is out of the scope of this paper. The genetic algorithm used in this work is implemented in the MATLAB software, according to [39]. The criteria described in the equations (28) and (31) are considered as the two conflicting objective functions which have to be minimized by the solving tool, by determining a trade-off between both objectives. Moreover, the algorithm must find solutions which ensure that the constraints described in equations (42)-(46) are not violated.

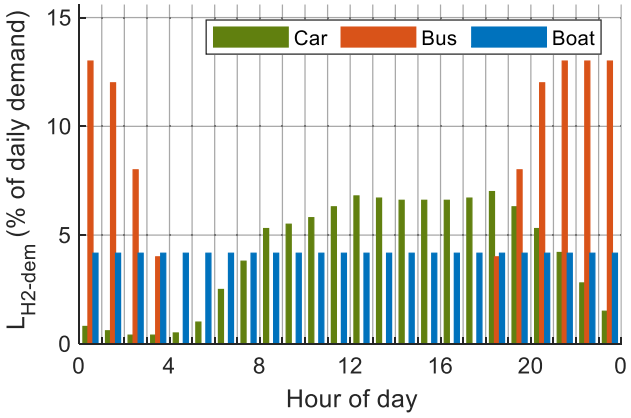

Fig. 6. Hourly distribution of the daily hydrogen demand for mobility uses.

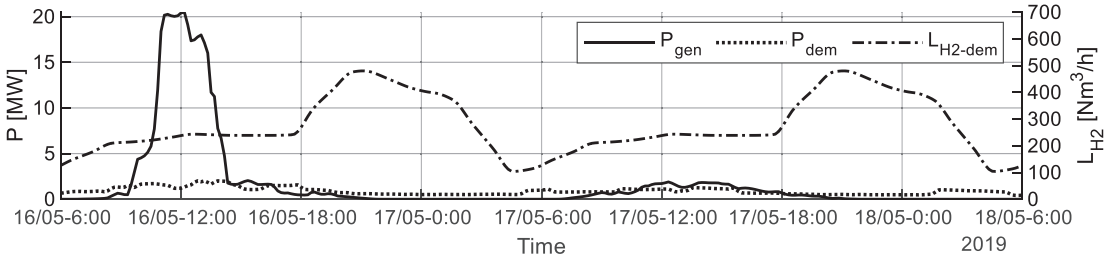

Fig. 5. Example of considered profiles (generated power, electrical load power and hydrogen load demand) for two days of the simulated year.

4. Results

The combined optimization for an industrial microgrid described in the Section 3 is applied to the case study of the harbour of Saint Nazaire (France). This scenario is based on a national ADEME project and seeks to develop the concept of Industrial Smart-Grid including collective self-consumption aspects. All the technical and economic parameters considered for this case study are given in the first subsection. Then, the results obtained for the sizing optimization are presented, and an example of operating profiles is shown for an optimal configuration. Finally, a sensitivity analysis for several economic parameters is carried out so as to show their impact on the sizing results.

4.1. Parameters and data

The technical parameters of the battery, the electrolyzer and the fuel cell are given in Table 1, in addition to the parameters related to the temporal simulation. The microgrid operation is simulated over a period of one year, considering the power generation and load demand data of 2019. The lower limits of the sizing decision variables ($C_{batref,low}$, $C_{H2ref,low}$, $P_{elzmax,low}$ and $P_{fcmax,low}$) are all set to zero, while the upper limits are set to: $C_{batref,up} = 20$ MWh, $C_{H2ref,up} = 20$ MWh, $P_{elzmax,up} = 20$ MW and $P_{fcmax,up} = 20$ MW.

The values considered for the economic parameters are given in Table 2, taken from different recent publications [30,40–44]. The profiles related to the selling and purchasing prices of electricity and hydrogen are presented in Fig. 4. The purchase price of electricity $c^{'}_{p-el}$ depends on the hour of the day (night tariff between 22 pm and 6 am, day tariff the rest of time) and the season (summer period: from 1st April to 31th October, winter period: from 1st November to 31th March). The selling price of electricity $c^{'}_{s-el}$ is related to the imbalance settlement price defined by electricity network operator in France (RTE) and varies according to the hour of the day [45], with values between 0.0291 €/kWh and 0.0566 €/kWh. The selling prices of hydrogen $c^{'}_{s-H2dem}$ and $c^{'}_{s-H2g}$ are considered to be constant whatever the hour of the day and the day of the year. The assumptions of $c^{'}_{s-H2dem} = 0.2$ €/kWh and $c^{'}_{s-H2g} = 0.1$ €/kWh are done, corresponding to probable values of the hydrogen market in the forthcoming years.

The electrical power generation profile P_{gen} considered in this case study involves the power generation from a PV array, for which the installed power is 4 MW, and the power generation from engine testing (genset) for which the power peak reaches 20 MW. The total amount of energy generated by both of these sources over a year amounts 10 GWh. The electrical power demand P_{dem} involves the load demand of industrial buildings and the seaport basin pumps. The maximum total load power demand reaches 3 MW and the annual demanded energy amounts to 6.5 GWh. A part of the considered profiles for the generated power P_{gen} and the electrical load power P_{dem} is given in Fig. 5, for two days of the considered year (2019).

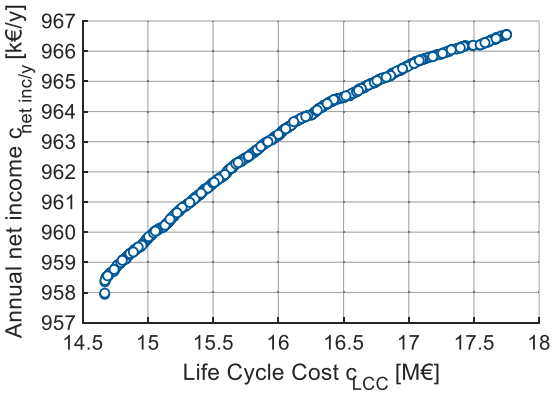

Fig. 7. Pareto front of the sizing optimization result.

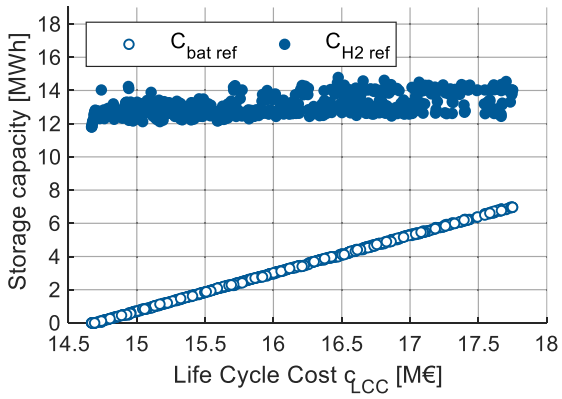

Fig. 8. Capacity of batteries and hydrogen tank of the Pareto front solutions.

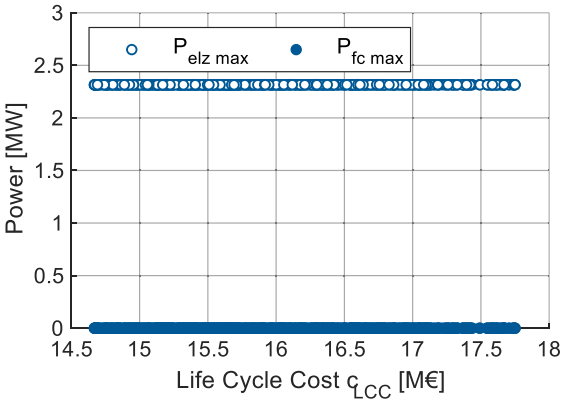

Fig. 9. Electrolyzer and fuel cell power of the Pareto front solutions.

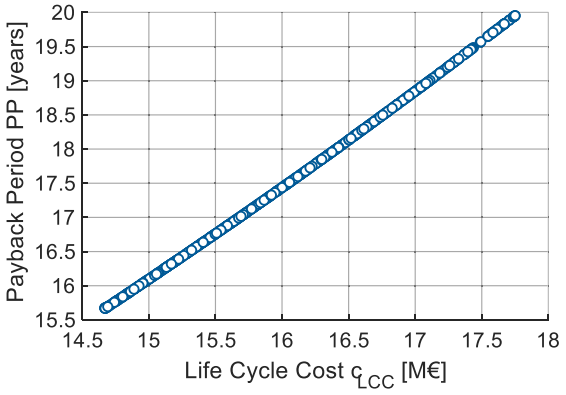

Fig. 10. Payback period of the Pareto front solutions.

The hydrogen load demand L_{H2-dem} considered in this study involves mobility needs and an industrial process (hydrogen engine testing). For the mobility needs, assumptions on the daily demand distribution have been done to build a typical daily load profile for each kind of mobility, as shown in Fig. 6. The profile related to the fueling of a fleet of cars is taken from [46] and the profile related to the fueling of a fleet of hydrogen buses is based on the data presented in [47]. Due to lack of available data in the literature, the hydrogen fueling profile of boats is more difficult to define. Thus, it is considered that the fueling of boats can occur whatever the hour of the day and the fueling events are equally distributed over the day, which leads to a constant demand over the day. The hypothesis considered for the simulations carried out in this

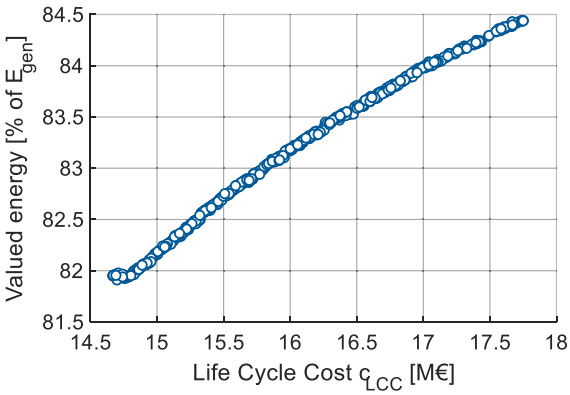

Fig. 11. Valued energy of the Pareto front solutions (in percent of total energy generated).

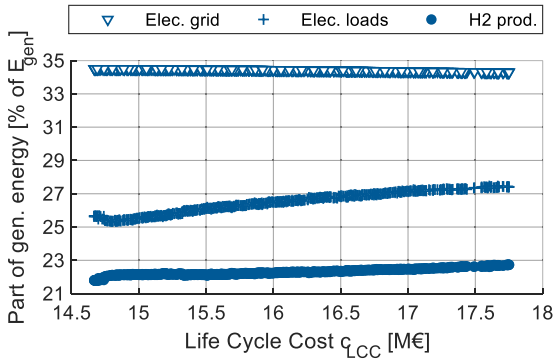

Fig. 12. Distribution of the valued energy for each solution of the Pareto front.

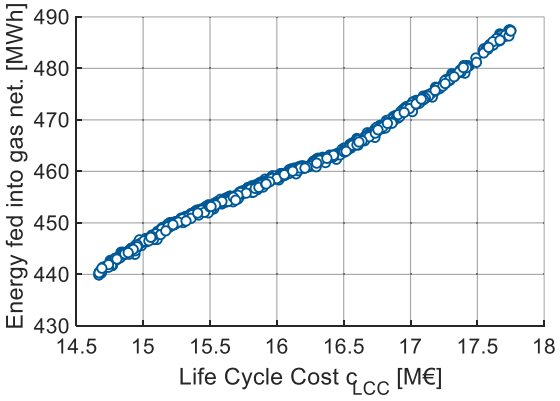

Fig. 13. Energy fed into gas network for each solution of the Pareto front.

section is that the daily hydrogen demand for each mobility use amounts 200 kgH_2/d, thus 7.292 GWh per year for the three kinds of mobility. For the hydrogen demand related to the industrial process, the annual demanded energy amounts 272 MWh, but this demand is unequally dispatched over the year (six weeks during the year). Considering these assumptions, an example of the total hydrogen demand profile L_{H2-dem} over two days is given in Fig. 5.

The parameters of the genetic algorithm used for the sizing optimization problem (NSGA-II) have been set after investigation of the most convenient values allowing a good compromise between accuracy and computing time. Thus, the number of individuals in a population has been set to 30 and the number of generations to 2000. The selection is based on tournament, the crossover rate has been set to 0.5 and the mutation rate to 0.1 [39]. The two-level optimization is performed using

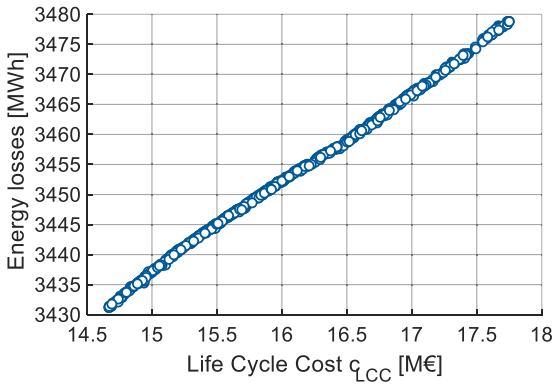

Fig. 14. Energy lost in conversion and storage systems for each solution of the Pareto front.

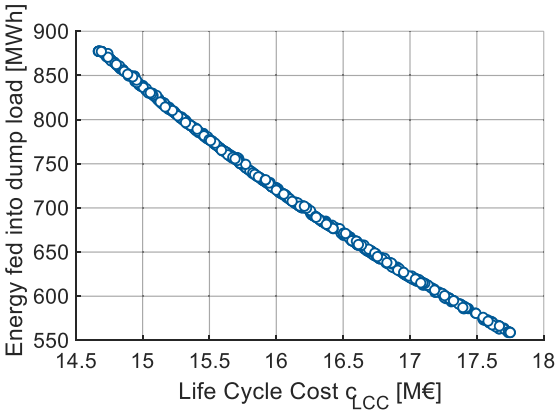

Fig. 15. Energy fed into the dump load for each solution of the Pareto front.

MATLAB 2020a software on an Intel® Core™ i9-9900U CPU @ 3.1 GHz processor, 128 GB RAM.

4.2. Sizing results

The Pareto front obtained for the sizing optimization is shown in Fig. 7. The results show that the solutions with a higher life cycle cost leads to a small increase of the annual net income, which means a higher investment brings little additional income. It can be noted that the obtained panel of solutions is limited in the right side by the maximum allowed payback period (20 years, for the point $c_{LCC} = 17.75$ M€). In the left side, the point for which the life cycle cost c_{LCC} amounts 14.7 M€ corresponds to the configuration necessary to allow the hydrogen load demand to be met (the corresponding life cycle cost includes the fixed investment costs of eq. (29)). The devices sizing of the different Pareto front solutions are plotted in Figs. 8 and 9. These results show that all the solutions present a similar hydrogen tank capacity (between 12 and 14 MWh) and electrolyzer power (2.3 MW). The spread of the solutions in the Pareto front is related to the increase of batteries capacity according to the increase of the life cycle cost, from 0 to 7 MWh. It can be noted that no fuel cell is included in the optimal configurations. This result can be explained by the high investment cost of a fuel cell and by the low efficiency of a power-to-gas-to-power system, leading to a low-profitable energy conversion compared to other ways of valorisation.

The payback period of the obtained solutions is given in Fig. 10. The payback period increases according to the increase of the life cycle cost, which indicates that a higher investment does not bring a sufficient income to decrease the payback period. However, the configurations with higher life cycle costs present a higher valued energy rate, as shown in Fig. 11. The valued energy corresponds to the quantity of the

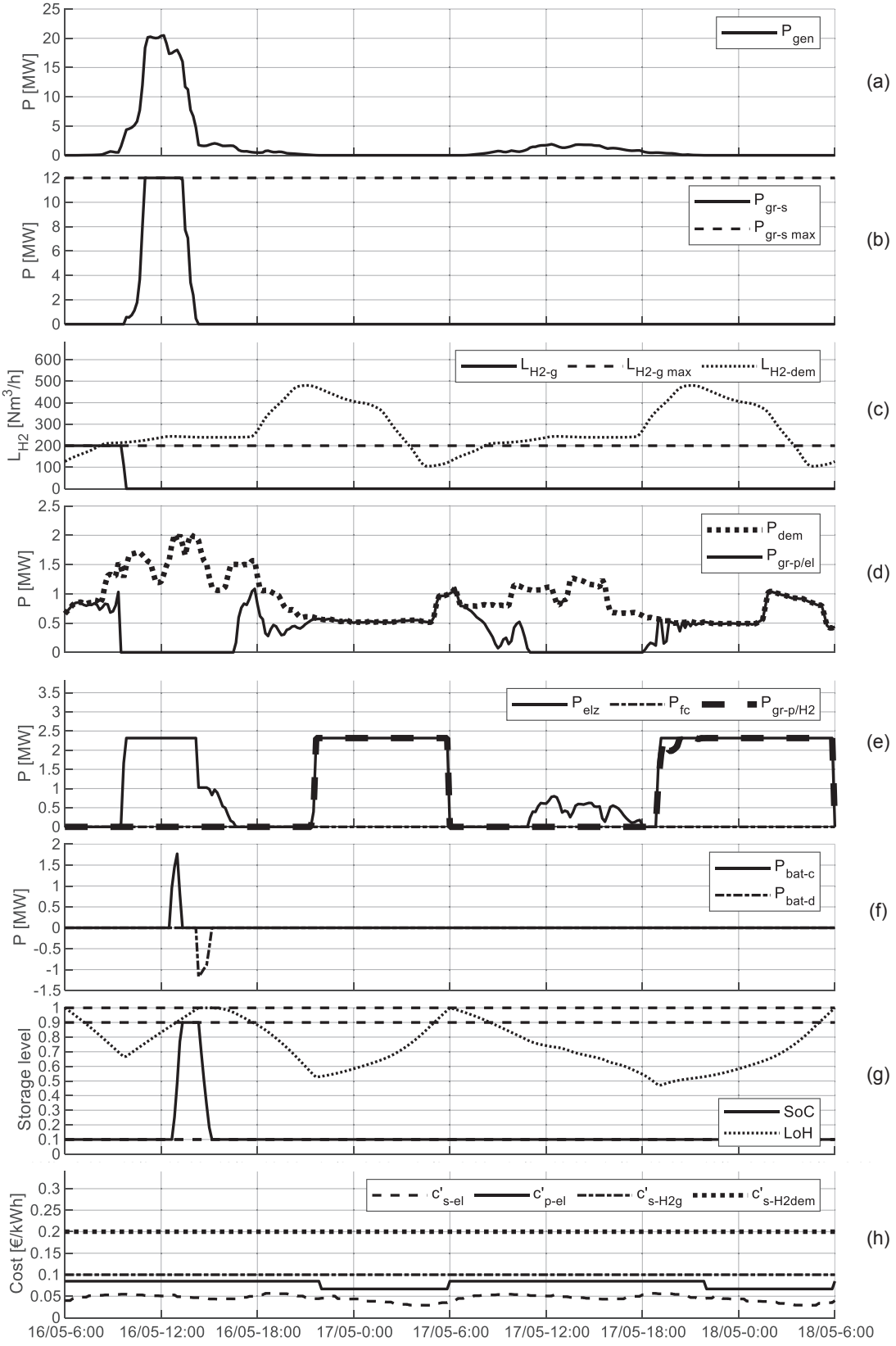

Fig. 16. Operating profiles of microgrid components for two days (From 2019 May 16th, 6am to May 18th, 6am).

generated energy which has been fed into the main grid, or used for the supply of electrical loads or converted into hydrogen. From this figure, the part of the generated energy which has been lost into batteries, electrolyzer and dump load can be deduced (between 18% and 15.5% of the generated energy). The corresponding distribution of the valued energy for each solution of the Pareto front is given in Fig. 12, according to the three ways of valorisation considered: the part of generated energy which is fed into the electrical network, the part transformed into hydrogen (after conversion by the electrolyzer) and the part used for the supply of the electrical loads. Most of the generated energy is fed into the electrical grid. Also, these results show that the energy used in self-consumption for the supply of the electrical loads raises according to the increase of the batteries capacity. As a consequence, the energy fed into the electrical network decreases, as it is more profitable to use the energy stored into the batteries in self-consumption than to feed it into the main grid. Moreover, the energy converted in hydrogen increases according to the increase of life cycle cost, corresponding to an increase of the hydrogen volume fed into the gas network (Fig. 13). It can be noted that the amount of electricity purchased for the supply of hydrogen loads decreases thanks to the increase of battery capacities, allowing the use of the generated energy to be postponed. Finally, it can be observed that the solutions with the highest life cycle cost values present more energy losses due to more frequent use of the batteries and the electrolyzer (Fig. 14), while less energy is fed into the dump load (Fig. 15) which could mean in a real case that less power curtailment would be necessary.

Thus, these results show that higher investments costs (corresponding here to the increase of the batteries capacity) allow the energy valorisation to be improved. A slight increase of the incomes can be obtained by avoiding the purchase of electricity for the supply of harbour loads (electrical and hydrogen loads).

Table 3
Economic results for 1 year simulation.

Cost category	Sub-cost	Result
Fixed expenses: Investment (CAPEX)	Batteries $c_{inv,bat}^{\cdot} C_{batref}$	0.35 M€
	Hydrogen tank $c_{inv,H2}^{\cdot} C_{H2ref}$	0.25 M€
	Electrolyzer $c_{inv,elz}^{\cdot} P_{elzmax}$	3.474 M€
	Fuel cell $c_{inv,fc}^{\cdot} P_{fcmax}$	0 M€
	PV $c_{inv,PV}$	4.366 M€
	Grid connection $c_{inv,gr}$	2 M€
	Dump load $c_{inv,dp}$	1.5 M€
	Total c_{invtot}	**11.94 M€**
Fixed expenses: Operational and maintenance expenditures (OPEX)	Batteries $c_{O\&M,bat}^{\cdot} C_{batref}$	6 k€/y
	Hydrogen tank $c_{O\&M,H2}^{\cdot} C_{H2ref}$	2.5 k€/y
	Electrolyzer $c_{O\&M,elz}^{\cdot} P_{elzmax}$	156 k€/y
	Fuel cell $c_{O\&M,fc}^{\cdot} P_{fcmax}$	0 k€/y
	PV $c_{O\&MPV}$	61.05 k€/y
	Total $c_{O\&Mtot/y}$	**225.9 k€/y**
Variable expenses	Batteries replacement $c_{repbat/y}$	3.13 k€/y
	Electrolyzer replacement $c_{repelz/y}$	356.45 k€/y
	Fuel cell replacement $c_{repfc/y}$	0 k€/y
	Electricity purchase for hydrogen production $c_{p-elH2/y}$	660.96 k€/y
	Electricity purchase for electrical loads supply $c_{p-eldem/y}$	353 k€/y
Annual incomes	Electricity sell $c_{s-el/y}$	173 k€/y
	Hydrogen sale for gas network $c_{s-H2g/y}$	44.28 k€/y
	Hydrogen sale for local demand $c_{s-H2dem/y}$	1513 k€/y
	Electrical load supply savings $c_{s-c/y}$	249.77 k€/y

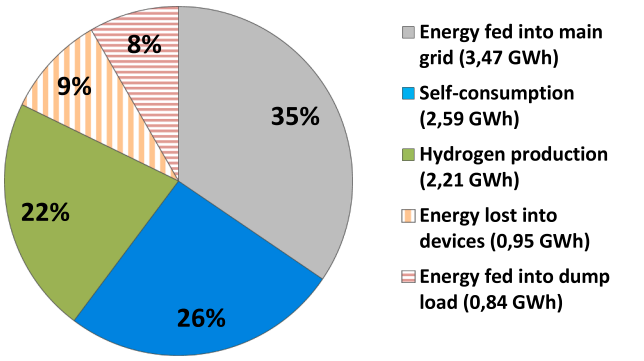

Fig. 17. Distribution of the total generated energy (10 GWh from engines testing and PV).

4.3. *Example of results for the energy management optimization (for a given optimal sizing)*

The operation of a configuration obtained from the Pareto front (Fig. 7) is analyzed in this section. The considered sizing is composed of: $C_{batref} = 1$ MWh, $C_{H2ref} = 12.5$ MWh, $P_{elzmax} = 2.3$ MW and $P_{fcmax} = 0$ MW, leading to an annual net income $c_{netinc/y} = 960$ k€/y and a life cycle cost $c_{LCC} = 15.12$ M€. The operating profile of each microgrid device is given in Fig. 16, over a period of two days (from May 16th, 2019 at 6am to May 18th, 2019 at 6 pm). Two kinds of behavior can be observed for the generated power during these two days (Fig. 16-a). During the first day, the electrical energy is generated from both solar photovoltaic panels and the engine testing process, whereas during the second day it is generated only by the solar photovoltaic panels. Thus, the generated power does not reach the same maximum value (20 MW for the 1st day vs. 2 MW for the 2nd day), involving differences on the energy valorisation. The recovered energy is used in priority for the most profitable solutions, which is the hydrogen production (Fig. 16-c and d) and if sufficient energy is available, for the supply of electrical loads allowing the purchase of electricity to be avoided (Fig. 16-d). In the case of a high generated power (thus for the days with the engine testing process), the surplus is fed into the electrical network (Fig. 16-b), as it happens between 10am and 2 pm during the first day of the displayed period. As the grid power limit is reached ($P_{gr-smax} = 12$ MW), a part of the generated power can be fed into the batteries (Fig. 16-g), so as to be used later for the supply of electrical loads (Fig. 16-d) and for H_2 production (Fig. 16-e). It can be noted that the maximum allowed *SoC* value is reached and the batteries charging is done as late as possible so as to minimize the energy losses due to self-discharge. The supply of hydrogen loads is done either by the discharge of the hydrogen tank (Fig. 16-g) or by the use of electrolyzer, for which the electrical power comes from the local energy sources or is drawn from the main grid (Fig. 16-e). It can be noted that the hydrogen tank is filled during the evening and the night, either by the microgrid energy sources or by electricity purchase to the main grid during the low-price period (from 10 pm to 6am, as shown in Fig. 16-h). As the self-discharge is higher for batteries than for hydrogen tank, the batteries are discharged before the hydrogen tank in order to limit the losses related to the self-discharge (Fig. 16-g). Thus, these results allow two trends to be distinguished, according to the economic hypotheses and the electrical power generation. So as to maximize the incomes, the harnessed energy is used in priority for the supply of electrical and hydrogen loads (the highest prices as shown in Fig. 16-h). Moreover, during the days where power generation from industrial machine testing happens, the harnessed energy can be fed into electrical and gas networks if a surplus of power exists (after considering the load supply).

This sizing is analyzed from an economic point of view in Table 3,

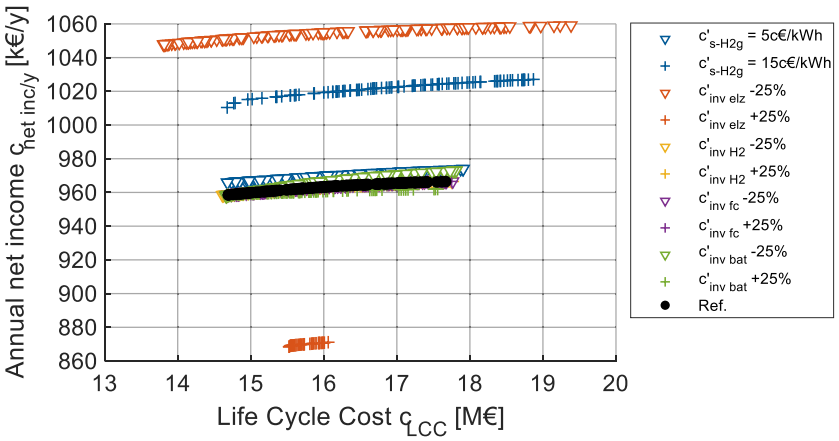

Fig. 18. Pareto fronts obtained for different economic hypotheses.

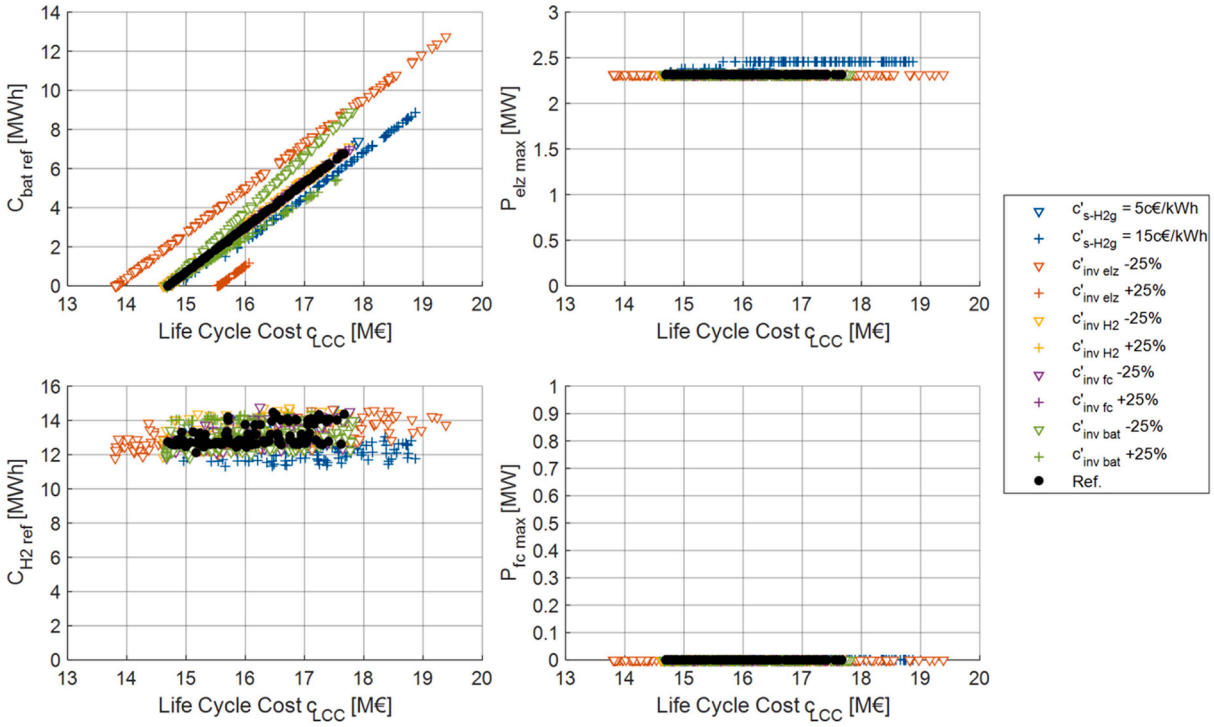

Fig. 19. Microgrid sizing of the obtained Pareto fronts for the sensitivity analysis.

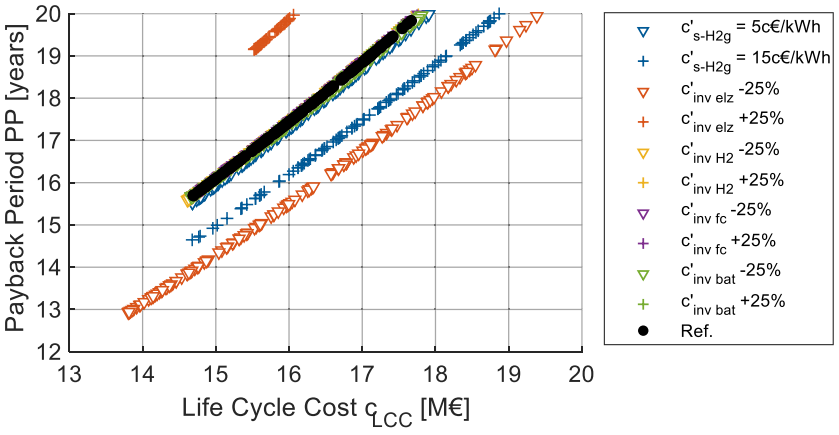

Fig. 20. Payback period of the obtained Pareto fronts for the sensitivity analysis.

according to the simulation results over one year data (2019). The solar photovoltaic panels and the electrolyzer represent most of the investment costs, respectively 36.5% and 29% of the total investment costs. Moreover, the obtained electrolyzer sizing involves high operational expenditures and must be replaced after 9 years as it is used most of the time (the hydrogen load demand must be met all the time). The incomes are mostly brought by the sale of hydrogen for the supply of seaport loads (among 76.4% of the total annual incomes), and then by the electricity savings (12.6%) and finally by the electricity fed into the main grid (8.7%). The hydrogen sale for gas network brought a little income (2.3%). These trends are related to the mismatch between energy selling and purchasing prices (Fig. 4). It can be noted that most of the purchased electricity is used for hydrogen production, since the power generated by the microgrid sources can be low.

Finally, an overall energy balance of this sizing is shown in Fig. 17, which gives the distribution of the use of the generated energy (10 GWh/y from engines testing and solar photovoltaic panels). It can be highlighted that 83% of the available energy is recovered, mostly thanks to the injection into the main grid as the power limit is high (12 MW). The rest of the recovered energy is shared between the supply of the electrical loads and the hydrogen production. Finally, these results show that 17% of the generated energy is lost, due to the losses in the battery and the electrolyzer and also due to the injection of the surplus into the dump load.

From the self-sufficiency point of view, it can be noted that 40% of the energy required by the electrical loads is supplied by the local energy sources (solar photovoltaic panels and engine testing). Moreover, the hydrogen produced thanks to these energy sources represents 27.6% of the total amount of produced hydrogen.

4.4. Sensitivity analysis

So as to show the impact of the economic hypotheses on the results, we present in this section a comparison of the Pareto front and the sizing obtained with different values of some economic parameters. The sensitivity of the results is performed for the investment costs and the selling price of hydrogen fed into the gas network. The investment costs are modified separately, by increasing or decreasing by 25% the reference values given in Table 2: $c^{'}_{inv,elz} = 1500$ €/kW, $c^{'}_{inv,H2} = 20$ €/kWh, $c^{'}_{inv,fc} = 2500$ €/kW and $c^{'}_{inv,bat} = 350$ €/kWh. Also, two values are considered for the sale price of the hydrogen injected into the gas network: $c^{'}_{s-H2g} = 0.05$ €/kWh then $c^{'}_{s-H2g} = 0.15$ €/kWh (the reference value is $c^{'}_{s-H2g} = 0.10$ €/kWh). The obtained Pareto fronts are presented in Fig. 18 and the corresponding optimal sizing is shown in Fig. 19. The payback period of all of these solutions is presented in Fig. 20. These results show that the most significant parameter is the investment cost of the electrolyzer, as a 25% decrease in this cost allows the annual net income obtained for the reference scenario to be increased by around 10% for a given life cycle cost value. This can be explained by the raise of batteries capacity (Fig. 19), allowing more energy to be used in self-consumption. Indeed, for a same life cycle cost value, the savings done by the decrease of electrolyzer investment cost can be used to buy more batteries, leading to higher incomes. A 25% increase of electrolyzer investment cost causes a 10% decrease in the annual net income for a given life cycle cost value, and a lower batteries capacity. The second most influent parameter is the selling price of hydrogen fed into the gas network. Indeed, if the selling price is raised to 15 c€/kWh, the annual net income is increased by around 6% for a given life cycle cost value. The consequences on the sizing are a higher electrolyzer power and a lower storage capacity (batteries and hydrogen tank), as it is more profitable to produce hydrogen and to fed it directly into the gas network than in the reference scenario. It can be noted that the reference value of 10 c€/kWh is not the best scenario due to the replacement cost of electrolyzer, which decreases the annual net income (the case with a 5 c€/kWh selling price leads to a lower replacement cost as the electrolyzer is less used, thus a higher annual net income). The third most influent parameter is the investment cost of the batteries. However, its influence is lower than those of the previous analyzed parameters, as only a 0.5% variation is observed on the annual net income values in comparison to the reference scenario. This can be explained by the change of batteries capacity (Fig. 19), which modifies the share of the generated energy, thus the incomes. Finally, it can be observed that the investment costs of the hydrogen tank and the fuel cell have little influence on the results, as the obtained fronts of solutions nearly coincide with the reference front. No fuel cell is used in the solutions, even if its investment cost would decrease. The results presented on Fig. 20 show that a decrease of the electrolyzer investment cost and a more expensive hydrogen selling price allows the payback period to be diminished by several months (up to two years) for a given life cycle cost value, in comparison to the reference scenario. Thus, the sensitivity analysis carried out show that the profitability of the solutions is mainly influenced by the investment costs of the electrolyzer and the batteries, in addition to the selling price of hydrogen fed into the gas network.

5. Conclusion

A combined optimization of the energy management and of the sizing of a multi-energy microgrid has been proposed in this paper. The case study of a seaport has been considered, but the methodology could be applied to any industrial multi-energy microgrid. The proposed methodology allows different technical and economic criteria to be taken into account, considering multiple electrical and hydrogen loads and multiple storage solutions. Thanks to the formulated objective function, the incomes can be maximized while the operational and investment costs are minimized. Among the multiple ways of energy valorisation considered, the hydrogen production appears to be the most profitable for the valorisation of the existing non-dispatchable energy sources in the area, thanks to the hydrogen selling price. Nevertheless, the energy can be sold to the main grid or used for the supply of the local electrical loads, so as to limit the high investment costs related to the electrolyzer and the hydrogen tank. The sensitivity analysis carried out in this paper has shown that the profitability of such microgrid depends mostly on the investment costs of the electrolyzer and the batteries and the selling price of hydrogen fed into gas network. Moreover, the aging of the devices must be considered as the replacement costs can represent a non-negligible part of the expenses, if the storage solutions are used frequently.

However, we can find some limits about the proposed optimization, which allows several perspectives to be considered. Firstly, it can be noted that the sizing optimization has been formulated according to real continuous decision variables. The next step could be to compare these results with those obtained with devices available on the market, so as to quantify the differences, considering an assembly of unit modules so as to get capacity and power as close as possible to the sizing results presented in this article. Also, a sizing optimization with discrete decision variables could be carried out, which would correspond to optimize the number of unit modules of each device. This will lead to solve a combinatorial optimization problem. Moreover, it can be noted that the economic assessment could be detailed by taking specific costs into account for each device, such as the replacement of specific components and the annual operational expenditure for example. Then, several perspectives deal with the system operation. The proposed energy management optimization involves the ability to forecast and to plan the power generation and the power demand over a period of several hours. However, some uncertainties exist and the operation of microgrids must be updated according to real-time decisions. Thus, the design of a real-time energy management system appears to be necessary, by proposing rule-based strategies and comparing their results with the optimal energy management strategy considered in this paper. Moreover, it could be interesting to integrate the electricity market mechanisms in the technical–economic model, by developing adapted energy management

rules. Then, the possible benefits could be quantified and also the impact on the sizing. An increase of the batteries capacity is expected, so as to provide ancillary services. Finally, some dedicated energy management strategies could be developed for the collective self-consumption, in order to define the energy sharing between multiple participants (producers and consumers) and the economic and operational model. Such studies have to be done according to the energy policy and the economic regulations expected in the incoming months for the hydrogen sale.

Funding

This research was funded by the french "Agence De l'Environnement et de la Maîtrise de l'Energie" (ADEME), Grant n°19PLC0149.

CRediT authorship contribution statement

Anthony Roy: Conceptualization, Formal analysis, Investigation, Methodology, Software, Validation, Visualization, Writing – original draft. **Jean-Christophe Olivier:** Conceptualization, Methodology, Supervision, Project administration, Funding acquisition. **François Auger:** Conceptualization, Methodology, Supervision, Project administration, Funding acquisition. **Bruno Auvity:** Conceptualization, Methodology, Supervision, Project administration, Funding acquisition. **Emmanuel Schaeffer:** Conceptualization, Methodology, Supervision, Project administration, Funding acquisition. **Salvy Bourguet:** Conceptualization, Methodology, Supervision, Project administration, Funding acquisition. **Jonathan Schiebel:** . **Jacques Perret:** Data curation, Resources.

Declaration of Competing Interest

The authors declare that they have no known competing financial interests or personal relationships that could have appeared to influence the work reported in this paper.

References

[1] Iris Ç, Lam JSL. A review of energy efficiency in ports: Operational strategies, technologies and energy management systems. Renew Sustain Energy Rev 2019;112:170–82. https://doi.org/10.1016/j.rser.2019.04.069.
[2] Kumar J, Kumpulainen L, Kauhaniemi K. Technical design aspects of harbour area grid for shore to ship power: State of the art and future solutions. Int J Electr Power Energy Syst 2019;104:840–52. https://doi.org/10.1016/j.ijepes.2018.07.051.
[3] Fang S, Wang Y, Gou B, Xu Y. Towards Future Green Maritime Transportation: An Overview of Seaport Microgrids and All-electric Ships. IEEE Trans Veh Technol 2019:1. https://doi.org/10.1109/TVT.2019.2950538.
[4] Trieste S, Hmam S, Olivier J-C, Bourguet S, Loron L. Techno-economic optimization of a supercapacitor-based energy storage unit chain: Application on the first quick charge plug-in ferry. Appl Energy 2015;153:3–14. https://doi.org/10.1016/j.apenergy.2015.04.054.
[5] Roy A, Auger F, Olivier J-C, Schaeffer E, Auvity B. Design, Sizing, and Energy Management of Microgrids in Harbor Areas: A Review. Energies 2020;13:5314. https://doi.org/10.3390/en13205314.
[6] Ahamad NBB, Su C-L, Zhaoxia X, Vasquez JC, Guerrero JM, Liao C-H. Energy Harvesting From Harbor Cranes With Flywheel Energy Storage Systems. IEEE Trans Ind Appl 2019;55:3354–64. https://doi.org/10.1109/TIA.2019.2910495.
[7] Skjong E, Volden R, Rødskar E, Molinas M, Johansen TA, Cunningham J. Past, Present, and Future Challenges of the Marine Vessel's Electrical Power System. IEEE Trans Transp Electrification 2016;2:522–37. https://doi.org/10.1109/TTE.2016.2552720.
[8] Samuelsen S, Shaffer B, Grigg J, Lane B, Reed J. Performance of a hydrogen refueling station in the early years of commercial fuel cell vehicle deployment. Int J Hydrog Energy 2020;45:31341–52. https://doi.org/10.1016/j.ijhydene.2020.08.251.
[9] Wu X, Li H, Wang X, Zhao W. Cooperative Operation for Wind Turbines and Hydrogen Fueling Stations With On-Site Hydrogen Production. IEEE Trans Sustain Energy 2020;11:2775–89. https://doi.org/10.1109/TSTE.2020.2975609.
[10] Mayer T, Semmel M, Guerrero Morales MA, Schmidt KM, Bauer A, Wind J. Techno-economic evaluation of hydrogen refueling stations with liquid or gaseous stored hydrogen. Int J Hydrog Energy 2019;44:25809–33. https://doi.org/10.1016/j.ijhydene.2019.08.051.
[11] Khani H, El-Taweel NA, Farag HEZ. Supervisory Scheduling of Storage-Based Hydrogen Fueling Stations for Transportation Sector and Distributed Operating Reserve in Electricity Markets. IEEE Trans Ind Inform 2020;16:1529–38. https://doi.org/10.1109/TII.2019.2926779.
[12] Song T, Li Y, Zhang X-P, Wu C, Li J, Guo Y, et al. Integrated port energy system considering integrated demand response and energy interconnection. Int J Electr Power Energy Syst 2020;117:105654. https://doi.org/10.1016/j.ijepes.2019.105654.
[13] Zia MF, Elbouchikhi EH, Benbouzid M. Microgrids energy management systems: A critical review on methods, solutions, and prospects. Appl Energy 2018;222:1033–55. https://doi.org/10.1016/j.apenergy.2018.04.103.
[14] Rigo-Mariani R, Chea Wae SO, Mazzoni S, Romagnoli A. Comparison of optimization frameworks for the design of a multi-energy microgrid. Appl Energy 2020;257:113982. https://doi.org/10.1016/j.apenergy.2019.113982.
[15] Li B, Roche R, Miraoui A. Microgrid sizing with combined evolutionary algorithm and MILP unit commitment. Appl Energy 2017;188:547–62. https://doi.org/10.1016/j.apenergy.2016.12.038.
[16] Li B, Roche R, Paire D, Miraoui A. Sizing of a stand-alone microgrid considering electric power, cooling/heating, hydrogen loads and hydrogen storage degradation. Appl Energy 2017;205:1244–59. https://doi.org/10.1016/j.apenergy.2017.08.142.
[17] Rullo P, Braccia L, Luppi P, Zumoffen D, Feroldi D. Integration of sizing and energy management based on economic predictive control for standalone hybrid renewable energy systems. Renew Energy 2019;140:436–51. https://doi.org/10.1016/j.renene.2019.03.074.
[18] Pan G, Gu W, Qiu H, Lu Y, Zhou S, Wu Z. Bi-level mixed-integer planning for electricity-hydrogen integrated energy system considering levelized cost of hydrogen. Appl Energy 2020;270:115176. https://doi.org/10.1016/j.apenergy.2020.115176.
[19] Molavi A, Shi J, Wu Y, Lim GJ. Enabling smart ports through the integration of microgrids: A two-stage stochastic programming approach. Appl Energy 2020;258:114022. https://doi.org/10.1016/j.apenergy.2019.114022.
[20] Sachs J, Sawodny O. Multi-objective three stage design optimization for island microgrids. Appl Energy 2016;165:789–800. https://doi.org/10.1016/j.apenergy.2015.12.059.
[21] Guo L, Liu W, Cai J, Hong B, Wang C. A two-stage optimal planning and design method for combined cooling, heat and power microgrid system. Energy Convers Manag 2013;74:433–45. https://doi.org/10.1016/j.enconman.2013.06.051.
[22] Rigo-Mariani R, Sareni B, Roboam X. Integrated Optimal Design of a Smart Microgrid With Storage. IEEE Trans Smart Grid 2017;8:1762–70. https://doi.org/10.1109/TSG.2015.2507131.
[23] Mahmoodi-k M, Montazeri M, Madanipour V. Simultaneous multi-objective optimization of a PHEV power management system and component sizing in real world traffic condition. Energy 2021;233:121111. https://doi.org/10.1016/j.energy.2021.121111.
[24] Montazeri-Gh M, Mahmoodi-K M. Optimized predictive energy management of plug-in hybrid electric vehicle based on traffic condition. J Clean Prod 2016;139:935–48. https://doi.org/10.1016/j.jclepro.2016.07.203.
[25] Madanipour V, Montazeri-Gh M, Mahmoodi-k M. Multi-objective component sizing of plug-in hybrid electric vehicle for optimal energy management. Clean Technol Environ Policy 2016;18:1189–202. https://doi.org/10.1007/s10098-016-1115-1.
[26] El-Taweel NA, Khani H, Farag HEZ. Hydrogen Storage Optimal Scheduling for Fuel Supply and Capacity-Based Demand Response Program Under Dynamic Hydrogen Pricing. IEEE Trans Smart Grid 2019;10:4531–42. https://doi.org/10.1109/TSG.2018.2863247.
[27] Maritime ports, infrastructure and transport - ESTUAIRE : Researching a multi-energy, multi-use smart grid for a port district n.d. https://www.pole-mer-bretagne-atlantique.com/en/maritime-ports-infrastructure-and-transport/project/2577 (accessed March 15, 2021).
[28] Ai B, Yang H, Shen H, Liao X. Computer-aided design of PV/wind hybrid system. Renew Energy 2003;28:1491–512. https://doi.org/10.1016/S0960-1481(03)00011-9.
[29] Bhandari B, Lee K-T, Lee G-Y, Cho Y-M, Ahn S-H. Optimization of hybrid renewable energy power systems: A review. Int J Precis Eng Manuf-Green Technol 2015;2:99–112. https://doi.org/10.1007/s40684-015-0013-z.
[30] Marocco P, Ferrero D, Gandiglio M, Ortiz MM, Sundseth K, Lanzini A, et al. A study of the techno-economic feasibility of H2-based energy storage systems in remote areas. Energy Convers Manag 2020;211:112768. https://doi.org/10.1016/j.enconman.2020.112768.
[31] Yao L, Damiran Z, Lim WH. Optimal Charging and Discharging Scheduling for Electric Vehicles in a Parking Station with Photovoltaic System and Energy Storage System. Energies 2017;10:550. https://doi.org/10.3390/en10040550.
[32] Mathworks. Mixed-integer linear programming (MILP) - MATLAB intlinprog n.d. https://fr.mathworks.com/help/optim/ug/intlinprog.html (accessed March 22, 2021).
[33] Erichsen G, Zimmermann T, Kather A. Effect of Different Interval Lengths in a Rolling Horizon MILP Unit Commitment with Non-Linear Control Model for a Small Energy System. Energies 2019;12:1003. https://doi.org/10.3390/en12061003.
[34] Marquant JF, Evins R, Carmeliet J. Reducing Computation Time with a Rolling Horizon Approach Applied to a MILP Formulation of Multiple Urban Energy Hub System. Procedia Comput Sci 2015;51:2137–46. https://doi.org/10.1016/j.procs.2015.05.486.
[35] Cao T, Hwang Y, Radermacher R. Development of an optimization based design framework for microgrid energy systems. Energy 2017;140:340–51. https://doi.org/10.1016/j.energy.2017.08.120.
[36] Janhunen E, Leskinen N, Junnila S. The Economic Viability of a Progressive Smart Building System with Power Storage. Sustainability 2020;12:5998. https://doi.org/10.3390/su12155998.

[37] Deb K, Pratap A, Agarwal S, Meyarivan T. A fast and elitist multiobjective genetic algorithm: NSGA-II - IEEE Journals & Magazine. IEEE Trans Evol Comput 2002;6:182–97.
[38] Tezer T, Yaman R, Yaman G. Evaluation of approaches used for optimization of stand-alone hybrid renewable energy systems. Renew Sustain Energy Rev 2017;73:840–53. https://doi.org/10.1016/j.rser.2017.01.118.
[39] Lin S. A NSGA-II Program in Matlab. Aerospace Structural Dynamics Research. Laboratory 2011.
[40] ADEME. Coûts des énergies renouvelables et de récupération en France - Données 2019. ADEME; 2020.
[41] IRENA. Electricity Storage Valuation Framework. International Renewable Energy Agency 2020.
[42] Gorre J, Ruoss F, Karjunen H, Schaffert J, Tynjälä T. Cost benefits of optimizing hydrogen storage and methanation capacities for Power-to-Gas plants in dynamic operation. Appl Energy 2020;257:113967. https://doi.org/10.1016/j.apenergy.2019.113967.
[43] Gorre J, Ortloff F, van Leeuwen C. Production costs for synthetic methane in 2030 and 2050 of an optimized Power-to-Gas plant with intermediate hydrogen storage. Appl Energy 2019;253:113594. https://doi.org/10.1016/j.apenergy.2019.113594.
[44] El-Taweel NA, Khani H, Farag HEZ. Optimal Sizing and Scheduling of LOHC-Based Generation and Storage Plants for Concurrent Services to Transportation Sector and Ancillary Services Market. IEEE Trans Sustain Energy 2020;11:1381–93. https://doi.org/10.1109/TSTE.2019.2926456.
[45] Imbalance settlement price - RTE Services Portal. Portail Serv RTE n.d. https://www.services-rte.com/en/learn-more-about-our-services/becoming-a-balance-responsible-party/Imbalance-settlement-price.html (accessed January 15, 2021).
[46] Kurtz J, Bradley T, Winkler E, Gearhart C. Predicting demand for hydrogen station fueling. Int J Hydrog Energy 2020;45:32298–310. https://doi.org/10.1016/j.ijhydene.2019.10.014.
[47] Doudard R. Flexibilité et interactions de long terme dans les systèmes multi-énergies : analyse technico-économique des nouvelles filières gazières et électriques en France. PhD Thesis. Paris Sciences et Lettres (ComUE) 2018.